18. M. Jandrot-Perrus, K. J. Clemetson, M. G. Huisse, M. C. Guillin, *Blood* **80**, 2781 (1992).
19. M. C. Bouton, C. Thurieau, M. C. Guillin, M. Jandrot-Perrus, *Thromb. Haemostasis* **80**, 310 (1998).
20. E. DeCandia *et al.*, *Thromb. Haemostasis* **77**, 735 (1997).
21. R. D. DeCristofaro, *J. Biol. Chem.* **275**, 3887 (2000).
22. C. Q. Li, A. Vindigni, J. E. Sadler, M. R. Wardell, *J. Biol. Chem.* **276**, 6161 (2001).
23. T. J. Rydel *et al.*, *Science* **249**, 277 (1990).
24. R. DeCristofaro, E. DeCandia, G. Croce, R. Morosetti, R. Landolfi, *Biochem. J.* **332**, 643 (1998).
25. L. DeMarco, M. Mazzucato, A. Masotti, Z. M. Ruggeri, *J. Biol. Chem.* **269**, 6478 (1994).
26. J. F. Dong, C. Q. Li, J. A. Lopez, *Biochemistry* **33**, 13946 (1994).
27. P. Marchese *et al.*, *J. Biol. Chem.* **270**, 9571 (1995).
28. C. M. Ward, R. K. Andrews, A. I. Smith, M. C. Berndt, *Biochemistry* **35**, 4929 (1996).
29. Y. Katagiri *et al.*, *Thromb. Haemostasis* **63**, 122 (1990).
30. J. Emsley, M. Cruz, R. Handin, R. Liddington, *J. Biol. Chem.* **273**, 10396 (1998).
31. S. Uff, J. M. Clemetson, T. Harrison, K. J. Clemetson, J. Emsley, *J. Biol. Chem.* **277**, 35657 (2002).
32. E. G. Huizinga *et al.*, *Science* **297**, 1176 (2002).
33. Materials and methods are available as supporting material on *Science* Online.
34. CCP4, *Acta Crystallogr. D* **50**, 760 (1994).
35. M. Jandrot-Perrus, M. G. Huisse, C. Ternisien, A. Bezeaud, M. C. Guillin, *Semin. Thromb. Haemostasis* **18**, 261 (1992).
36. Z. R. Gan, Y. Li, Z. Chen, S. D. Lewis, J. A. Shafer, *J. Biol. Chem.* **269**, 1301 (1994).
37. J. H. Wang, *Trends Biochem. Sci.* **27**, 122 (2002).
38. L. Shapiro *et al.*, *Nature* **374**, 327 (1995).
39. M. C. Berndt, Y. Shen, S. M. Dopheide, E. E. Gardiner, R. K. Andrews, *Thromb. Haemostasis* **86**, 178 (2001).
40. C. Ravanat *et al.*, *Thromb. Haemostasis* **83**, 327 (2000).
41. A. Nicholls, GRASP; Columbia University, New York, 1993.
42. E. F. Workman, G. C. White, R. L. Lundblad, *J. Biol. Chem.* **252**, 7118 (1977).
43. J. Dumas *et al.*, in preparation.
44. We thank E. Presman for growth of CHO cells, T. McDonagh for assistance with GpIbα purification, J. Rouse for mass spectrometry, G. Shaw for comments on the manuscript, and J. Bard and G. McDermott for the assistance with data collection. The coordinates for the GpIbα-thrombin complex have been deposited in the Protein Data Bank with the accession code 1P8V.

Supporting Online Material
www.sciencemag.org/cgi/content/full/301/5630/222/DC1
Materials and Methods
SOM Text
Figs. S1 and S2
References

26 February 2003; accepted 23 May 2003

5-HT$_{4(a)}$ Receptors Avert Opioid-Induced Breathing Depression Without Loss of Analgesia

Till Manzke,[1]* Ulf Guenther,[2]* Evgeni G. Ponimaskin,[1] Miriam Haller,[1] Mathias Dutschmann,[1] Stephan Schwarzacher,[3] Diethelm W. Richter[1]†

Opiates are widely used analgesics in anesthesiology, but they have serious adverse effects such as depression of breathing. This is caused by direct inhibition of rhythm-generating respiratory neurons in the Pre-Boetzinger complex (PBC) of the brainstem. We report that serotonin 4(a) [5-HT$_{4(a)}$] receptors are strongly expressed in respiratory PBC neurons and that their selective activation protects spontaneous respiratory activity. Treatment of rats with a 5-HT$_4$ receptor–specific agonist overcame fentanyl-induced respiratory depression and reestablished stable respiratory rhythm without loss of fentanyl's analgesic effect. These findings imply the prospect of a fine-tuned recovery from opioid-induced respiratory depression, through adjustment of intracellular adenosine 3′,5′-monophosphate levels through the convergent signaling pathways in neurons.

Serotonin (5-hydroxytryptamine, or 5-HT) is an important neurotransmitter that is involved in a wide range of neuromodulatory processes in the central nervous system, by acting on a number of different 5-HT receptor isoforms (*1*, *2*). The 5-HT$_4$ receptor is a recently identified subtype that is widely and abundantly expressed as alternatively spliced variants in various brain regions (*3*–*5*). The receptor exerts excitatory effects through its positive coupling to heterotrimeric Gs proteins to activate adenylyl cyclases and to induce robust increases of intracellular adenosine 3′,5′-monophosphate (cAMP) levels (*6*, *7*). The receptor also couples to G13 proteins to activate small guanosine triphosphates of the Rho family (*8*) (Fig. 1A).

Recent cloning of the 5-HT$_4$ receptor (*9*) initiated the development of 5-HT receptor subtype–specific immunocytochemistry and pharmacology. We produced a specific antibody against a synthetic peptide that corresponds to the C-terminal sequence of the 5-HT$_{4(a)}$ receptor's isoform (amino acids His^{364} to Pro^{380}) (*10*) (Fig. 1B), which allowed us to specifically identify the spatial expression of the 5-HT$_4$ receptors in the central nervous system, including the brainstem (*11*). We found that 5-HT$_4$ receptors are abundantly expressed in the Pre-Boetzinger complex (PBC), a region in the lower brainstem that is known to generate and control spontaneous breathing movements (*12*).

This specific antibody was also used to analyze the coexpression of the 5-HT$_{4(a)}$ receptor with μ-opioid receptors and Substance P–reactive neurokinin-1 (NK-1) receptors, which have been suggested as potential immunocytochemical markers for respiratory neurons (*13*–*15*). Medullary motoneurons were visualized by choline acetyl transferase (ChAT) staining and excluded from the analysis (*16*). In multiple-labeling experiments (with NK-1 receptors, 5-HT$_{4(a)}$ receptors, and ChAT), we identified three different types of immunoreactive medullary interneurons: 35.5% of immunoreactive interneurons displayed intense NK-1 and 5-HT$_{4(a)}$ receptor co-immunoreactivities and 34.1% of interneurons revealed 5-HT$_{4(a)}$ receptor immunoreactivity alone, whereas 30.4% of interneurons revealed only NK-1 receptor immunoreactivity (Fig. 2, A and B) (supporting online text). In a similar study, the brainstem was analyzed for co-immunoreactivities of μ-opioid and 5-HT$_{4(a)}$ receptors within the PBC region, a region essential for respiratory rhythm generation (*12*). We found positive staining in 46.8% of interneurons for both μ-opioid and 5-HT$_{4(a)}$ receptors, whereas a population of 53.2% of interneurons exhibited only μ-opioid receptor immunoreactivity (Fig. 2C) (supporting online text). These data suggest that approximately one-half of all 5-HT$_{4(a)}$ receptor–positive interneurons in the PBC region coexpress both NK-1 receptors and μ-opioid receptors. We confirmed this by multiple staining of 5-HT$_{4(a)}$, NK-1, and μ-opioid receptors in the same slice (fig. S1) as well as by reverse transcription–polymerase chain reaction (RT-PCR) analysis.

To verify that the 5-HT$_{4(a)}$ receptor–immunoreactive interneurons indeed represent respiratory neurons, single-cell RT-PCR analysis was performed on the cytosol of identified inspiratory neurons in the rhythmically active slice preparation (Fig. 3) (*17*). We found that 95.2% of the neurons analyzed expressed 5-HT$_4$ receptors (Fig. 3B) (supporting online text). In view of the large number of 5-HT$_4$ receptor isoforms, it was of particular interest to analyze the expression of the different 5-HT$_4$ receptor splice variants. RT-PCR analysis of the PBC region and of individual respiratory neurons proved the expression of

[1]Department of Neuro- and Sensory Physiology, University of Goettingen, Humboldtallee 23, 37073 Goettingen, Germany. [2]Center of Anesthesiology, University of Goettingen, Robert-Koch Street 40, 37075 Goettingen, Germany. [3]Department of Anatomy, Kreuzbergring 36, 37075 Goettingen, Germany.
*These authors contributed equally to this work.
†To whom correspondence should be addressed. E-mail: d.richter@gwdg.de

5-HT$_{4(a)}$, 5-HT$_{4(b)}$, and 5-HT$_{4(f)}$ receptor mRNA, but not of 5-HT$_{4(e)}$ receptor mRNA, in the PBC region (Fig. 3B) (*16*), whereas defined inspiratory neurons expressed only the 5-HT$_{4(a)}$ mRNA (Fig. 3B). Immunocytochemical studies confirmed these observations, demonstrating a strong 5-HT$_{4(a)}$ receptor immunoreactivity in biocytin-labeled inspiratory neurons (Fig. 3C).

We also determined, by single-cell RT-PCR, the expression profile for NK-1 receptor mRNA as well as for the μ-opioid receptor mRNA (*16*). Expression of the NK-1 receptor mRNA was found in only 30.7% of defined inspiratory neurons, whereas immunohistochemical data from the PBC region indicated NK-1 receptor expression in 65.9% of PBC neurons (Fig. 2). This difference revealed the presence of nonrespiratory neurons that express NK-1 (*18*). In contrast, μ-opioid receptor mRNA was detected in all inspiratory neurons analyzed, which is in line with immunocytochemical data reported by other laboratories (*13*). Our data demonstrate that 5-HT$_{4(a)}$ and μ-opioid receptor–mediated signaling pathways are coexistent in inspiratory neurons (Fig. 1A) and therefore are capable of interacting in an antagonistic manner; μ-opioid receptors operate through Gi/o proteins to decrease the cAMP levels (*19*), and 5-HT$_{4(a)}$ receptors counteract by activating Gs proteins to raise cAMP concentration (*7*).

The physiological significance of such potential interaction between 5-HT$_{4(a)}$ and μ-opioid receptor–mediated signaling in the regulation of respiration was further explored in the in vivo–like perfused rat brainstem–spinal cord preparation (*16*, *20*), which contains the fully intact respiratory network, and finally verified in the live rat. First, we tested the effects of the 5-HT$_{4(a)}$ receptor–specific agonistic drug BIMU8 (*10*) on ongoing respiratory activity and found that vascular application of this drug significantly increased phrenic nerve activity at all doses tested (concentration range: 0.3 to 10 μM) (Fig. 4A). The whole-animal experiments verified that application of BIMU8 (1 to 2 mg/kg) significantly increased respiratory minute volume (RMV) in vivo (supporting online text). This stimulatory effect was 5-HT$_4$ receptor–specific, because it was blocked by the specific antagonist GR 113808 in both experimental approaches (supporting online text). Involvement of 5-HT$_4$/Gs signaling in the regulation of respiratory activity was confirmed by the findings that application of dibutyryl-cAMP increased phrenic nerve activity, whereas application of the adenylyl cyclase blocker SQ 22,536 decreased phrenic nerve activity. Coactivation of 5-HT$_3$ receptors by BIMU8 could be excluded, because these receptors are not functionally expressed in respiratory neurons (*21*, *22*)

The physiological consequences of μ-opioid receptor activation were tested with the specific agonist fentanyl. Fentanyl is a synthetic opioid widely used for anesthesia

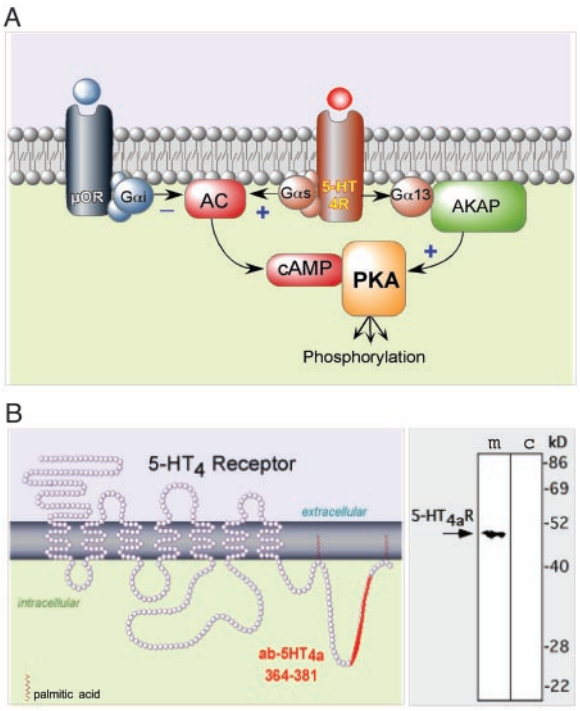

Fig. 1. (**A**) Schematic illustration of the signal transduction pathways mediated by 5-HT$_4$ and μ-opioid receptors. Whereas 5-HT$_4$ receptors stimulate adenylyl cyclases (ACs) through both Gs and G13 proteins, μ-opioid receptors inhibit AC activities through a Gi/o-mediated inhibitory pathway. μOR, μ-opioid receptor; Gαi, Gαs, and Gα13, the α_i, α_s, and α13 subunits of heterotrimeric G protein; 5-HT 4R, 5-HT$_4$ receptor; AKAP, A-kinase anchor protein; PKA, protein kinase A. (**B**) Western blot analysis of the brainstem lysate with a polyclonal antibody raised against the C-terminal part of the 5-HT$_{4(a)}$ receptor isoform. Left: Model of the 5-HT$_{4(a)}$ receptor with the amino acids CHSGHHQELEKLPIHNDP (red) (*27*) used for the production of an antibody (ab). Right: Membrane (m) and cytosolic (c) fractions prepared from the lysate of the rat brainstem were separated by SDS–polyacrylamide gel electrophoresis and then subjected to Western blotting with an antibody to the 5-HT$_{4(a)}$ receptor.

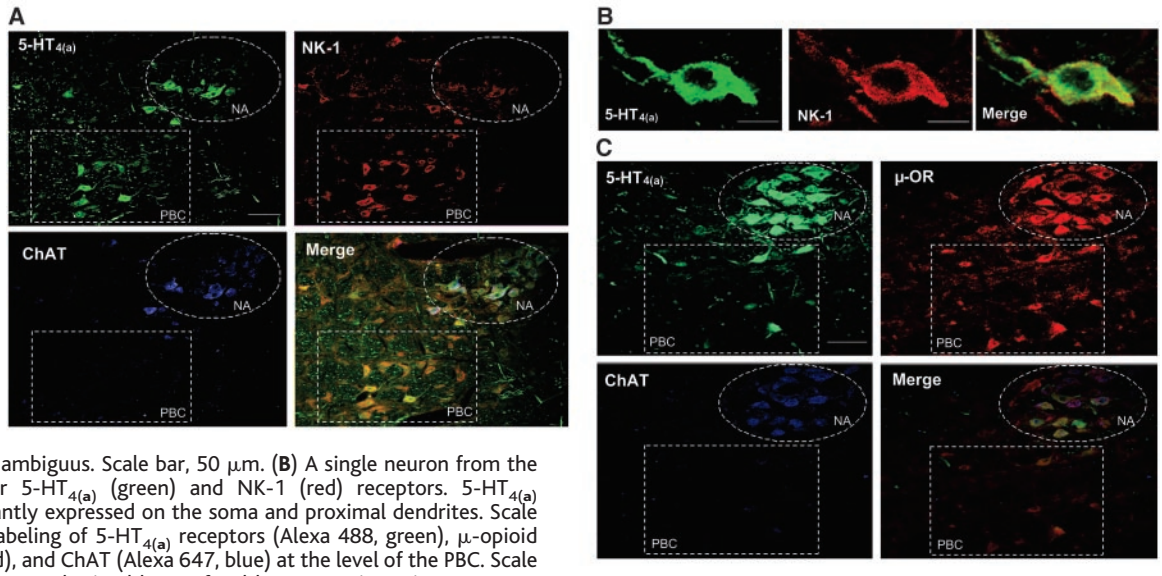

Fig. 2. Distribution of 5-HT$_{4(a)}$, NK-1, and μ-opioid receptor and ChAT immunoreactivities within the ventrolateral region of the brainstem that contains the PBC. (**A**) Triple-labeling with appropriate antibodies of a 40-μm-thick transversal slice cut at the level of the PBC, showing 5-HT$_{4(a)}$ receptors (Alexa 488, green), NK-1 receptors (Alexa 546, red), and ChAT (Alexa 647, blue). NA, Nucleus ambiguus. Scale bar, 50 μm. (**B**) A single neuron from the PBC region, stained for 5-HT$_{4(a)}$ (green) and NK-1 (red) receptors. 5-HT$_{4(a)}$ receptors are predominantly expressed on the soma and proximal dendrites. Scale bar, 10 μm. (**C**) Triple-labeling of 5-HT$_{4(a)}$ receptors (Alexa 488, green), μ-opioid receptors (Alexa 546, red), and ChAT (Alexa 647, blue) at the level of the PBC. Scale bar, 50 μm. All images were obtained by confocal laser scanning microscopy.

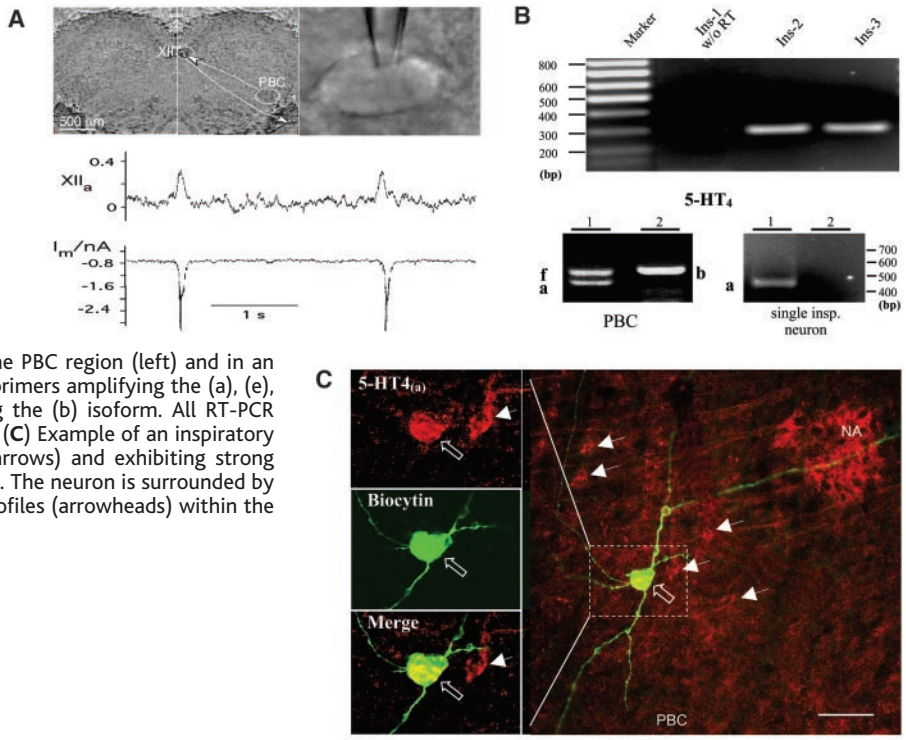

Fig. 3. Expression of 5-HT$_4$ receptors in functionally identified inspiratory neurons. (**A**) Top: The site of electrophysiological recordings (left) with an inspiratory neuron on the tip of the patch pipette (right). Traces: Integrated hypoglossal nerve (XII$_a$) activity (middle) corresponds to rhythmic inward currents in a single inspiratory neuron recorded in the whole-cell configuration (bottom). I_m, membrane current. (**B**) Top: Single-cell RT-PCR analysis of inspiratory neurons. Gel electrophoresis was carried out for RT-PCR products amplified with 5-HT$_4$ primers. The control reaction without reverse transcription is shown in the first line. Ins, inspiratory neuron; bp, base pairs. Bottom: RT-PCR analysis of 5-HT$_4$ receptor splice variants in the PBC region (left) and in an individual inspiratory neuron (right). Lane 1 shows primers amplifying the (a), (e), and (f) isoforms. Lane 2 shows primers amplifying the (b) isoform. All RT-PCR products were evaluated by direct DNA sequencing. (**C**) Example of an inspiratory PBC neuron labeled intracellularly with biocytin (arrows) and exhibiting strong 5-HT$_{4(a)}$ receptor immunoreactivity (Alexa 546, red). The neuron is surrounded by 5-HT$_{4(a)}$ receptor immunoreactivities on somatic profiles (arrowheads) within the PBC. Scale bar, 50 μm.

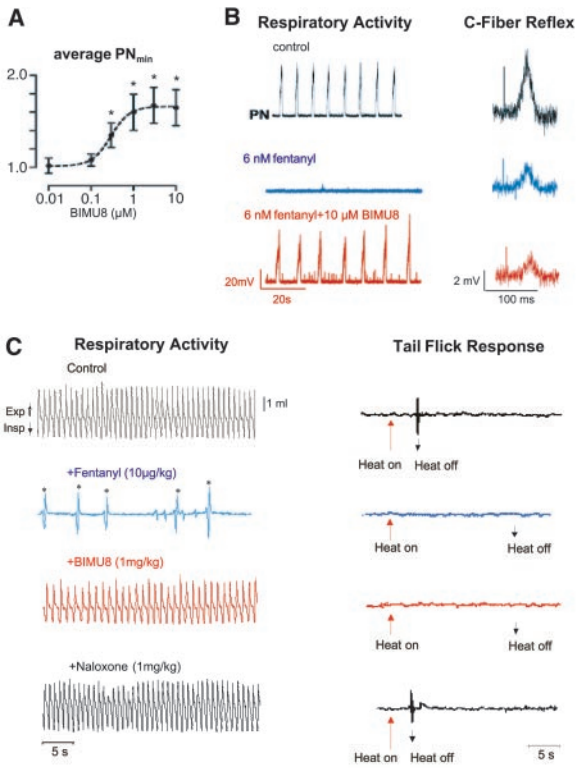

Fig. 4. Stimulation of 5-HT$_4$ receptors by the selective agonist BIMU8 removes opioid-induced respiratory depression without loss of the antinociceptive effect of opioids in [(A) and (B)] the perfused brainstem preparation, as well as in (C) the intact in vivo rat. (**A**) The dose-dependent effect of BIMU8 on phrenic nerve minute activity (PNA$_{min}$) (*16*). Statistically significant changes from untreated controls are indicated by asterisks ($P < 0.05$). (**B**) Left: Application of fentanyl (blue) caused a marked depression of PNA$_{min}$ by 91.2 ± 4.2% ($n = 8$, $P < 0.05$) as compared with a control (black). In three cases, fentanyl even led to apnea. Respiratory activity was reestablished by a subsequent application of BIMU8 (red) in a dose-dependent manner (*16*). Right: Responses of the spinal CFR. The black trace represents the CFR of the untreated control. Application of fentanyl (blue) suppressed the CFR by 60.9 ± 6.5% ($n = 8$, $P < 0.01$). Subsequent administrations of BIMU8 (red) did not affect opioid-induced depression of the CFR (*16*). (**C**) Left: Respiratory airflow in an anesthetized, spontaneous-breathing, in vivo rat. Application of 10 to 15 μg/kg fentanyl (blue) induced a marked reduction in RMV to 3.9 ± 8.5% of control RMV ($n = 5$, $P < 0.001$). Consecutive application of 1 to 2 mg/kg BIMU8 (red) prevailed over this effect of fentanyl and restored stable breathing, with RMV recovering to 70.6 ± 18.1% ($n = 5$, $P < 0.001$) of control RMV (*16*). Application of naloxone reestablished respiratory activity to the control level. Asterisks indicate transient periods of artificial ventilation, which were necessary to rescue the animal during genuine fentanyl treatment. Exp, expiration; Insp, inspiration. Right: Analysis of nociception based on the TFR. A quick TFR was obtained in control conditions (black), which was completely abolished after application of fentanyl (blue). This absence of analgetic response remained unchanged after subsequent administration of BIMU8 (red). Application of naloxone (1 mg/kg) immediately reestablished the TFR (supporting online text).

and for the relief of acute and chronic pain, although it produces serious adverse reactions, such as hypoventilation (*19*, *23*, *24*). Application of fentanyl to the perfused rat brainstem–spinal cord preparation induced the expected antinociceptive effects, as seen by a 60.9 ± 6.5% ($n = 8$, $P < 0.01$) reduction of the C-fiber reflexes (CFRs) (Fig. 4B). At the same time, however, respiratory activity was almost completely suppressed (Fig. 4B). In three cases, exposure to fentanyl led to apnea that would have been lethal under normal conditions. The effects obtained in in vivo animals were even more pronounced. Here, fentanyl produced strong antinociceptive effects that resulted in a complete abolishment of the tail flick response (TFR) (Fig. 4C). However, as in the brainstem preparation, spontaneous respiratory movements were completely blocked (Fig. 4C) (supporting online text).

Therefore, we tested whether activation of the 5-HT$_4$ receptor–mediated signaling pathway is effective in overcoming fentanyl-induced respiratory depression and apnea (Fig. 4B) (*19*, *25*). To verify the power of 5-HT$_4$ receptors in restoration of respiratory activity, we performed successive applications of fentanyl and of BIMU8. The crucial result was that consecutive applications of BIMU8 indeed reestablished stable respiratory activity within 3 min in the perfused brainstem preparation (Fig. 4B) (supporting online text). This effect was fully reproduced in vivo. In the latter cases, subsequent application of BIMU8 (1 to 2 mg/kg) overcame the fentanyl-induced ap-

nea and restored stable breathing, with RMV recovered to 70.6 ± 18.1% within 3 min (Fig. 4C) (supporting online text).

Lastly, we investigated whether 5-HT_4 receptor stimulation obliterates the nociceptive function of opioids. We tested CFRs in the brainstem–spinal cord preparation and the TFR in vivo (*16*). Application of BIMU8 after fentanyl treatment was sufficient to reestablish stable respiration in both test systems without any significant effects on the CFRs (Fig. 4B) or the TFR (Fig. 4C). Additional application of naloxone (1 mg/kg) immediately reestablished the TFR (Fig. 4C). The absence of BIMU8-induced effects on nociception can be explained by the finding that dorsal horn spinal interneurons reveal abundant μ-opioid but not 5-$HT_{4(a)}$ receptor immunoreactivity (fig. S2).

This study provides evidence that activation of 5-HT_4 receptors in neurons of the medullary respiratory center represents a method for the treatment of respiratory depression induced by opioids. Stimulation of 5-HT_4 receptors effectively counteracts fentanyl-induced respiratory depression without compromising its antinociceptive potency. An inspiring possibility is that application of 5-HT_4 receptor agonists could be used for the treatment of critical respiratory events caused by fentanyl in postoperative situations and for the treatment of pain patients against overdose of opioids (*23*). In essence, a straightforward therapy that targets convergent intracellular signal pathways by means of a receptor-specific pharmacology (*26*) might open strategies for effective treatment in a wide spectrum of critical clinical situations.

References and Notes

1. D. Hoyer *et al*., *Pharmacol. Rev*. **46**, 157 (1994).
2. S. Hynie, *Cesk. Fysiol*. **44**, 135 (1995).
3. V. Compan *et al*., *Eur. J. Neurosci.* **8**, 2591 (1996).
4. M. T. Vilaro *et al*., *Brain. Res. Mol. Brain. Res*. **43**, 356 (1996).
5. M. T. Vilaro *et al*., *Neuropharmacology* **42**, 60 (2002).
6. J. Bockaert, M. Sebben, A. Dumuis, *Mol. Pharmacol*. **37**, 408 (1990).
7. M. Heine *et al*., *Pfluegers Arch*. **443**, 418 (2002).
8. E. G. Ponimaskin *et al*., *J. Biol. Chem*. **277**, 20812 (2002).
9. S. Claeysen *et al*., *FEBS Lett*. **398**, 19 (1996).
10. E. G. Ponimaskin *et al*., *Biochem. J*. **353**, 627 (2001).
11. T. Manzke *et al*., *FENS Forum Abstr*. **1**, 77 (abstr. 022.9) (2002).
12. J. C. Smith *et al*., *Science* **254**, 726 (1991).
13. P. A. Gray *et al*., *Science* **286**, 1566 (1999).
14. P. A. Gray *et al*., *Nature Neurosci*. **4**, 927 (2001).
15. P. G. Guyenet, H. Wang, *J. Neurophysiol*. **86**, 438 (2001).
16. Materials and methods are available as supporting material on *Science* Online.
17. J. C. Smith, K. Ballanyi, D. W. Richter, *Neurosci. Lett*. **134**, 153 (1992).
18. Y. W. Li, P. G. Guyenet, *Am. J. Physiol*. **273**, 805 (1997).
19. K. Ballanyi *et al*., *J. Physiol*. **504**, 127 (1997).
20. J. F. Paton, *J. Neurosci. Methods* **65**, 6 (1996).
21. D. Morin, S. Hennequin, R. Monteau, G. Hilaire, *Brain Res*. **535**, 281 (1990).
22. D. W. Richter *et al*., *Neuroscientist* **6**, 181 (2000).
23. E. B. Dunn, J. J. Wolfe, *Vet. Hum. Toxicol*. **42**, 36 (2000).
24. S. Takeda *et al*., *Anesthesiology* **95**, 740 (2001).
25. M. Denavit-Saubie, J. Champagnat, W. Zieglgansberger, *Brain Res*. **155**, 55 (1978).
26. D. W. Richter *et al*., *Respir. Physiol*. **110**, 113 (1997).
27. Single-letter abbreviations for the amino acid residues are as follows: A, Ala; C, Cys; D, Asp; E, Glu; F, Phe; G, Gly; H, His; I, Ile; K, Lys; L, Leu; M, Met; N, Asn; P, Pro; Q, Gln; R, Arg; S, Ser; T, Thr; V, Val; W, Trp; and Y, Tyr.

28. Supported by the medical faculty of the University of Gœttingen and by the Deutsche Forschungsgemeinschaft (Sonderforschungsbereich 406 and grant no. PO732/1-1).

Supporting Online Material

www.sciencemag.org/cgi/content/full/301/5630/226/DC1
Materials and Methods
SOM Text
Figs. S1 and S2
References and Notes

18 March 2003; accepted 4 June 2003

Neuronal Correlates of Goal-Based Motor Selection in the Prefrontal Cortex

Kenji Matsumoto,* Wataru Suzuki, Keiji Tanaka

Choosing an action that leads to a desired goal requires an understanding of the linkages between actions and their outcomes. We investigated neural mechanisms of such goal-based action selection. We trained monkeys on a task in which the relation between visual cues, action types, and reward conditions changed regularly, such that the monkeys selected their actions based on anticipated reward conditions. A significant number of neurons in the medial prefrontal cortex were activated, after cue presentation and before motor execution, only by particular action-reward combinations. This prefrontal activity is likely to underlie goal-based action selection.

During purposeful behavior, a goal may first come to mind, requiring the retrieval of the action that will realize this goal as its outcome. Alternatively, sensory cues may activate multiple action plans, one of which has to be selected by its linkage to the current goal (*1*, *2*). The neural mechanisms of such goal-based action selection have not been studied systematically, although studies with monkeys (*3*–*11*) and humans (*12*–*15*) have demonstrated that activity in the prefrontal cortex (PFC) conveys information about rewards or goals. We trained monkeys on a task in which they were able to select an action based on goal, and we recorded the activity of cells from the medial and lateral parts of PFC. These two parts of PFC are thought to play essential roles in cognitive control of behavior (*16*–*21*).

The task was a visually cued, asymmetrically rewarded GO/NO-GO task with reversals (Fig. 1A) (*21*). One of two visual cues was presented, and after a delay the monkey either performed a GO response (pulling and returning the joystick) or a NO-GO response (holding the joystick) (noted as NG), depending on the cue. After another delay, a liquid reward was provided only after correct GO responses or correct NG responses (noted as reward +). Fixation was required throughout the trial. Within a single block of trials, the relations between visual, motor, and reward variables were fixed, and only two visual-motor-reward (VMR) combinations were provided. Between blocks, the combinations were changed by reversing the visual-motor or visual-reward relation. All eight possible VMR combinations (Fig. 1B) were covered in four blocks of trials, which were run while we recorded the activity of a single cell in PFC, so that the effect of each variable on neuron activity could be distinguished. After 4 to 6 months of training on reversals (*22*), the monkeys were able to reattain a high performance level rather quickly, usually with fewer than eight errors, after a reversal of motor requirement or reward condition.

The monkeys selected motor responses based on the anticipation of reward conditions, as opposed to exclusively using stimulus-motor associations. The linkages between visual stimuli and reward conditions, between motor responses and reward conditions, and between stimuli and motor responses, were fixed within a block, so it is conceivable that the monkeys memorized these linkages over the course of a block of trials. Therefore, the monkeys may have selected their motor responses using stimulus-motor associations alone. However, they may also have selected correct motor responses using memory of stimulus-reward and motor-reward linkages (*23*). Behavioral data showed that the anticipation of reward condition played an essential role in selection of motor response. The monkeys were more likely to break eye-

Cognitive Brain Mapping Laboratory, RIKEN Brain Science Institute, 2-1 Hirosawa, Wako, Saitama 351-0198, Japan.

*To whom correspondence should be addressed. E-mail: matsumot@postman.riken.go.jp